EPR and optical investigation of europium doped $Ba_{12}F_{19}Cl_5$

1999 J. Phys.: Condens. Matter 11 7301

(http://iopscience.iop.org/0953-8984/11/38/309)

J. Phys.: Condens. Matter **11** (1999) 7301–7309. Printed in the UK PII: S0953-8984(99)05235-2

EPR and optical investigation of europium doped $Ba_{12}F_{19}Cl_5$

J M Rey, H Bill†, D Lovy and F Kubel‡

Département de Chimie Physique, Sciences II, 30 quai E Ansermet, 1211 Genève 4, Switzerland

E-mail: hans.bill@chiphy.unige.ch

Received 16 June 1999

Abstract. Single crystals of the new host $Ba_{12}F_{19}Cl_5$ doped with Eu^{2+} were grown and studied by electron paramagnetic resonance (EPR) and luminescence emission spectroscopy. Three different Eu^{2+} sites were observed. Two of them had orthorhombic point symmetry while the last one was monoclinic. Physico-chemical and symmetry arguments allowed us to establish correspondence between the different Eu^{2+} centres and the host cation lattice sites. All three centres presented in their ground state important crystal field splitting. The 80 K luminescence emission spectrum consisted of one broad unsymmetrical f–d band peaking at 22 700 cm^{-1}. No 4f–4f transitions of the Eu^{2+} ion were observed between room temperature and 80 K.

1. Introduction

Alkaline earth fluorohalides and fluorides are important host materials for rare-earth ions (REIs) in view of their use as solid state lasers [1]. Many of these matrices doped with transition metal ions (TMIs) [2] further proved to have model character for the investigation of magnetic and optical properties of the impurities. Mixed matlockites containing Sm^{2+} were the first materials to show reversible and stable optical hole-burning at room temperature [3]. Another important aspect is the photo-stimulated luminescence (PSL) exhibited by the BaFBr compound doped with Eu^{2+} (see e.g. [4–6] and references therein). This enabled its use in imaging screens for two-dimensional x-ray radiography [7]. Another much less investigated aspect of these materials is that several of this class present luminescence emission properties of considerable practical interest when doped with TMI or REI. Though much practical knowledge has accumulated in this field there is still much research to be done on specific systems, in particular on fundamental issues regarding structures and mechanisms involved in the high efficiency emitters.

Recent studies of the (BaF_2–$BaCl_2$) phase diagram brought new compounds [8, 9] which show new and promising optical properties as hosts for RE impurities. Details of the structure of the local REI complexes have to be known for advanced insight into the REI–host interactions involved in the excitation transfer. In particular this involves acquiring knowledge of the location of the RE ion and the influence of the ligand field on the electronic structure. For these reasons, a detailed spectroscopic study of the europium impurity in the new host was undertaken. This paper presents results on the crystal growth and on the electron paramagnetic resonance (EPR) and optical luminescence spectroscopy of this ion (ground state $^8S_{7/2}$) in the

† Author to whom correspondence should be addressed.

‡ Present address: Professor F Kubel, Technische Universität Wien, Inst. für Mineralog., Kristallogr. und Strukturchem., Getreidemarkt 9, Vienna, Austria.

0953-8984/99/387301+09$30.00

$Ba_{12}F_{19}Cl_5$ host. This compound crystallizes in the non-centrosymmetric hexagonal space group $P\bar{6}2m$ (No 189) with $a = b = 1408.48$ and $c = 427.33$ pm [8].

2. Experiment

Single crystals of $Ba_{12}F_{19}Cl_5$ were grown using either the Bridgman or the Czochralski method. The $Ba_{12}F_{19}Cl_5$ samples used for the EPR and optical experiments were doped with 1 mol‰ of EuF_2. The starting materials, BaF_2 (Merck, suprapure), $BaCl_2$ (Merck, suprapure, dried at 180 °C under high vacuum) and EuF_2 (Cerac, 99.9% pure), were handled in an oxygen- and water-free ($p_{O_2} < 10$ ppm) glove box. In a typical Czochralski run, 0.2 mol of BaF_2, 0.2 mol of BaFCl (pre-crystallized from BaF_2 and $BaCl_2$) together with the EuF_2 were melted (1100 °C) in a pyrolitic graphite crucible under 0.2 atm of argon (quality 5N7). The nominal temperature of the crucible was lowered to about 975 °C before starting the pulling at approximately 0.5 mm h^{-1}. A typical size of the single crystals obtained was $5 \times 5 \times 3$ mm^3. The samples used for the EPR and optical experiments were oriented with the aid of a polarizing microscope and by the Laue x-ray technique.

The EPR spectra were obtained at 36 GHz on a home-built superheterodyne Ka-band spectrometer with low temperature equipment of our design. Data analysis and the computer simulations were performed with our SPINHAM program [10]. Luminescence and optical excitation measurements were carried out with a home-built spectrophotometer already described elsewhere [10].

3. Results

3.1. EPR experiments

Most of the EPR spectra were recorded at 78 K. But a few experiments were performed at 4.2 K to determine the absolute signs of the b_1^m parameters. Three mutually independent Eu^{2+} EPR spectra were observed. The associated europium sites are denoted in the following No 1, No 2 and No 3 respectively. The spectrum recorded with the magnetic field $\boldsymbol{B}$ parallel to the a crystal axis is shown in figure 1. It consists of groups of seven fine-structure lines ($S = 7/2$), each with a typical full width at half maximum (FWHM) of about 400 MHz. This quite large FWHM is mainly a consequence of the unresolved hyperfine structure due to the isotopes ^{151}Eu and ^{153}Eu. As the overall spectrum is complex, it was necessary to study its angular variation in several crystallographic planes and with an angular increment of only 2.5°. The angular variation obtained with $\boldsymbol{B} \parallel (ab)$ evidently reflects the hexagonal symmetry of the crystal. The angular variations with $\boldsymbol{B} \parallel (ac)$ and $\boldsymbol{B} \parallel (b^*c)$, respectively, show that (ab) is a mirror plane for all three sites. Thus when $\boldsymbol{B} \parallel c$ each site will contribute one set of seven lines whereas when $\boldsymbol{B} \parallel a$ each one will produce two sets.

Site No 1 presented its maximum fine structure splitting with $\boldsymbol{B} \parallel a$. The stick-diagram labelled (1) in figure 1 marks the corresponding set of EPR lines. The experimental angular variations of this spectrum obtained when $\boldsymbol{B}$ was rotated in the (ab) and (ac) planes are given in figures 2(a) and 2(b), respectively. These two plots show that (ac) and (ab) *are* mirror planes. Thus the Eu^{2+} centre No 1 has orthorhombic symmetry with the maximum splitting of its EPR spectrum parallel to an a axis.

Site No 2 gave an experimental angular variation of the EPR spectrum in the (ab) plane which is presented in figure 3. For clarity, only the $(M_J \rightarrow M'_J) = 5/2 \rightarrow 3/2$ and $-3/2 \rightarrow -5/2$ transitions are shown there. The extremum of the fine structure splitting was observed at $\pm 4.7°$ from the a axis. As before, the stick-diagram (labelled 2) in figure 1

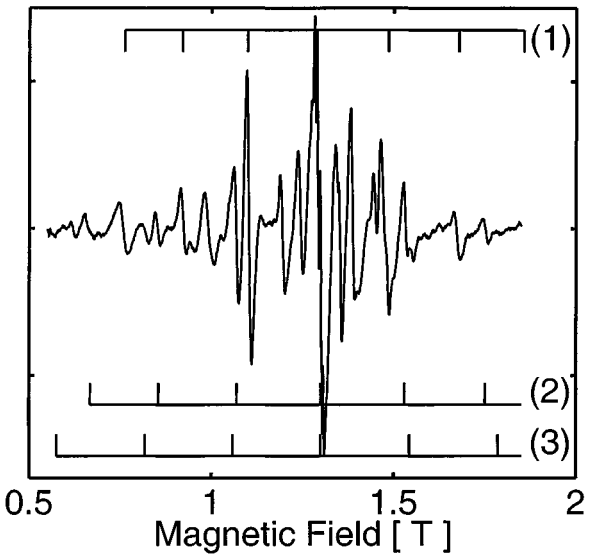

Figure 1. Ka-band global EPR spectrum of $Ba_{12}F_{19}Cl_5$:Eu (1‰) with $\boldsymbol{B} \parallel a$ ($T = 78$ K, $\nu = 36$ GHz). Each centre produces two spectra. The stick-diagrams (1), (2) and (3), respectively, label the spectrum with the larger splitting for each of the three (see text).

marks only the set of lines of this spectrum showing strongest splitting. The angular variations in the (ac) and (b^*c) planes further demonstrated that only (ab) is a mirror plane for this site. The Eu^{2+} centre No 2 has thus monoclinic symmetry with a maximum splitting in the (ab) plane, at $\pm 4.7^\circ$ from the a axis.

Site No 3 produced an EPR signal of comparatively lower intensity. The EPR lines corresponding to this site are labelled by the stick-diagram 3 in figure 1. In spite of the low intensity it was possible to follow the angular variation of the lines near the principal axis of the crystal field tensor. The result is that the largest fine structure splitting was observed for $\boldsymbol{B} \parallel a$ and that (ac) and (ab) are mirror planes. Thus, the Eu^{2+} centre No 3 has orthorhombic symmetry with the principal crystal field axis along a.

3.1.1. Parametrization. Due to the very complex angular variations of the overall spectrum, the detailed symmetry analysis presented above was mandatory before useful spin Hamiltonian parameters could be determined. The further procedure used is already described elsewhere [10]. The angular variations of the orthorhombic sites, No 1 and No 3, were parametrized with the following spin Hamiltonian:

$$H = g\beta_0 \boldsymbol{B} \cdot \boldsymbol{S} + (b_2^0 O_2^0 + b_2^2 O_2^2) + (b_4^0 O_4^0 + b_4^2 O_4^2 + b_4^4 O_4^4). \tag{1}$$

For the monoclinic site (No 2), the spin Hamiltonian was:

$$H = g\beta_0 \boldsymbol{B} \cdot \boldsymbol{S} + (b_2^0 O_2^0 + b_2^1 O_2^1 + b_2^2 O_2^2) + (b_4^0 O_4^0 + b_4^1 O_4^1 + b_4^2 O_4^2 + b_4^3 O_4^3 + b_4^4 O_4^4). \tag{2}$$

The O_1^m represent Steven's operator equivalents [11, 12] and the other symbols have their usual meaning. Formally, the b_6^m terms have to be included. But as the spectral components have typical FWHM of 400 MHz the residual error of approximately 150 MHz/point was already attained by fitting equations (1) and (2) to the angular variations. The inclusion of the b_6^m terms resulted in marginal improvement of the fit and the values obtained were zero within the error limits. The EPR lines corresponding to site No 3 were weaker, and fewer points were available

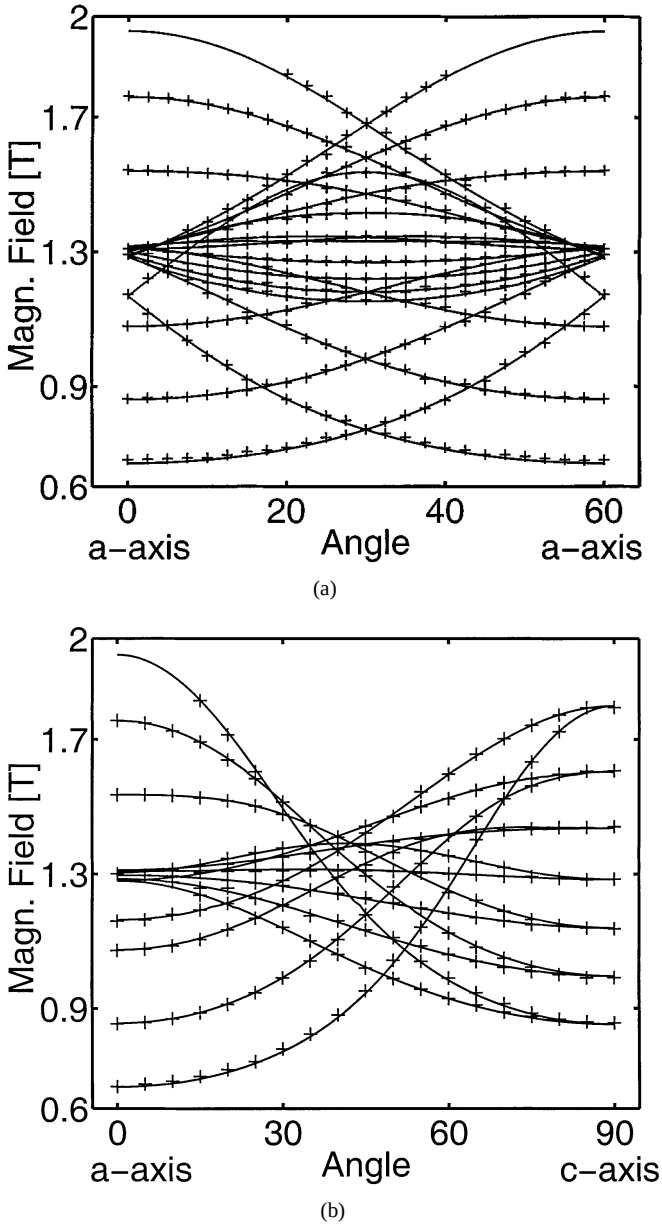

Figure 2. Experimental angular variations of the Ka-band EPR spectrum for site No 1 (crosses) ($T = 78$ K, $\nu = 36$ GHz) (a) in the (ab) plane and (b) in the (ac) plane. The full lines represent the results of the simulation (see text).

for the parametrization. The inclusion of the b_2^0 and b_2^2 terms was sufficient to describe the spectrum near the principal axis.

The constants of the corresponding spin Hamiltonian were obtained for each site with the aid of this optimization procedure. The results are given in table 1. The indicated errors correspond to the variation needed to increase the residual error of the fits by a factor of 2. Some of the parameters (for e.g. b_4^2 of site No 2) showed an important error margin. But setting

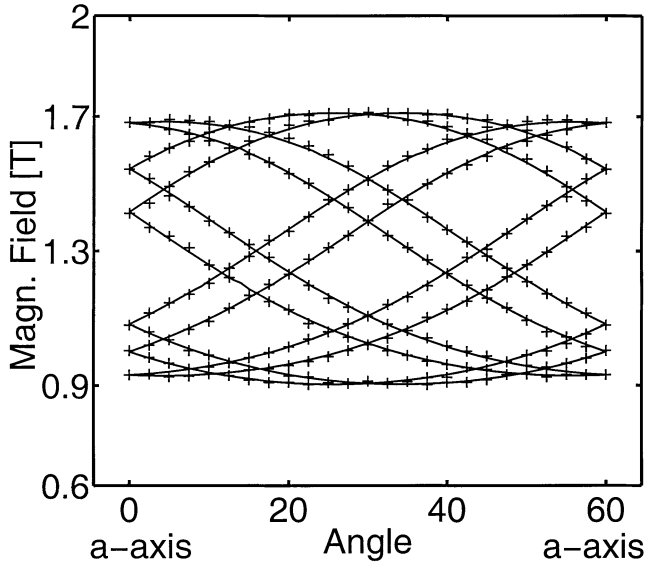

Figure 3. Experimental angular variation in the (ab) plane of the $M_J = 5/2 \rightarrow 3/2$ and $M_J = -3/2 \rightarrow -5/2$ EPR lines for site No 2. The full lines represent the results of the simulation for these levels (see text). ($T = 78$ K, $\nu = 36$ GHz).

Table 1. Spin-Hamiltonian parameters (in 10^{-4} [cm^{-1}]) for the Eu^{2+} EPR centres in $Ba_{12}F_{19}Cl_5$ at 78 K.

	No 1	No 2	No 3
$g_{isotropic}$	1.987 (8)	1.989 (12)	1.990 (12)
b_2^0	-340 ± 7	296 ± 9	-374 ± 6
b_2^1	—	2.1 ± 55	—
b_2^2	148 ± 14	343 ± 19	59 ± 13
b_4^0	0.16 ± 0.13	-0.11 ± 0.16	—
b_4^1	—	0.46 ± 1.9	—
b_4^2	0.14 ± 0.57	-0.17 ± 0.98	—
b_4^3	—	0.71 ± 5.8	—
b_4^4	-0.22 ± 0.90	0.33 ± 1.3	—
Angle[a] (°)	0	±4.7(5)	0

[a] Angle between the a crystal axis and the z axis of the local EPR referential. The EPR x axis is parallel to the c crystal axis.

them to zero distinctly decreased the quality of the fit. The absolute sign of the crystal field parameters was determined by analysing the relative intensities at 4.2 K. Theoretical angular variations were calculated with the aid of equations (1) and (2) and by using the constants of table 1. The results are shown as full lines in figures 2 and 3. The b_2^0 and b_2^2 parameters were the most important ones for all three Eu^{2+} centres. This was often observed in low symmetry complexes [2, 10, 13].

3.2. Optical experiments

Optical emission and excitation spectra were obtained at room temperature and at ∼80 K from the same $Ba_{12}F_{19}Cl_5$:Eu (1‰) samples previously studied by EPR. The 80 K emission spectrum

(excited at 31 200 cm^{-1}) is presented in figure 4(a). It exhibited one broad unsymmetrical band with unresolved structure, with a maximum at 22 700 cm^{-1}. The excitation spectrum at 80 K (detected at 24 700 cm^{-1}) (figure 4(a)) consisted of three large structures (maxima: 29 700, 36 200, 40 900 cm^{-1}) formed by several partly resolved bands. Efforts to identify Eu^{3+} in these crystals gave negative results.

4. Discussion

4.1. EPR experiments

Three different barium environments are present in the pure $Ba_{12}F_{19}Cl_5$ structure [8]. All have coordination number nine as shown in figure 5.

Cluster (A) (see figure 5(a)) has point symmetry group C_{2v} and is formed by five fluorine and four chlorine ions surrounding the barium ion. Four fluorine ions (2 F2 and 2 F3) form a rhombus which can be considered as the base of the cluster whereas the four chlorine ions (4 Cl1) subtend above the Ba ion a larger rectangle rotated by 45° around the axis. The last fluorine ion (F5) located on the C_2 axis is capping the chlorine frame. It has the shortest Ba–F distance (250 pm). This arrangement around the barium ion is similar to the one found in the BaFCl structure [14]. But note that the local point symmetry of the barium ion in this last mentioned host is C_{4v}.

The barium ion of cluster (B) has C_{2v} point symmetry too (figure 5(b)). The structural differences between this cluster and (A) are that here the frame forming the base is heavily deformed as it consists of two fluorine (2 F2) and two chlorine ions (2 Cl1) in *trans* positions whereas the second one consists of only fluorine ions (4 F1). The fluorine ion F4 caps this latter frame and is on the C_2 symmetry axis.

The lower symmetry C_s of cluster (C) (figure 5(c)) with respect to (A), (B) is due to the fact that the 'upper' distorted rhomboid is made up by two fluorine (2 F4) and two chlorine ions (2 Cl2) in *cis* positions whereas the base consists of four fluorine ions (F1, 2 F2 and F3). The fluorine ion (F1) caps the former frame. The mirror plane is parallel to (ab) and contains the ions F3, 2 F1 and Ba.

The experimental fact that in many alkaline earth halide and double halide hosts the Eu^{2+} ion introduced as an impurity always occupies the cationic lattice sites is well established (see e.g. [2, 15–18]). This is in agreement with ionic radius and iso-charge arguments. The present EPR results demonstrate that this rule is fulfilled here too. Indeed, the Eu^{2+} sites No 1 and No 3 have orthorhombic symmetry, as do the Ba^{2+} sites of clusters (A) and (B) of the perfect $Ba_{12}F_{19}Cl_5$ structure. For this reason we assign the EPR centres No 1 and No 3 to Eu^{2+} located on these cation lattice sites. Note that the C_{2v} symmetry does not impose identical positions of the Eu^{2+} and the Ba^{2+} as the only constraint for the Eu^{2+} is to stay on the C_2 axis. Therefore a slightly displaced position of this ion is expected. Symmetry arguments alone cannot decide whether centre No 1 or No 3 corresponds to the (A) site etc. To clarify this point more experiments e.g. ENDOR would be needed. The remaining EPR centre, No 2, has monoclinic symmetry. We assign this one to Eu^{2+} located on (C) cluster host cation lattice sites. Of course, a shifted position (in the C_s plane) of this impurity is again expected.

Common to the three Eu^{2+} centres is their sizeable ground state crystal field splitting. In particular the b_2^0 parameter is much more important than the corresponding quantity observed in BaFCl:Eu^{2+} [15] where $b_2^0 = 11.4 \times 10^{-4}$ [cm^{-1}]. As the symmetry around the Eu^{2+} ions is lower in $Ba_{12}F_{19}Cl_5$, there is no evident partial compensation between 'cubic' and 'axial' contributions to the ligand field. Therefore the strong host dependence of b_2^0 observed [16] in the matlockite-type hosts does not seem to apply here.

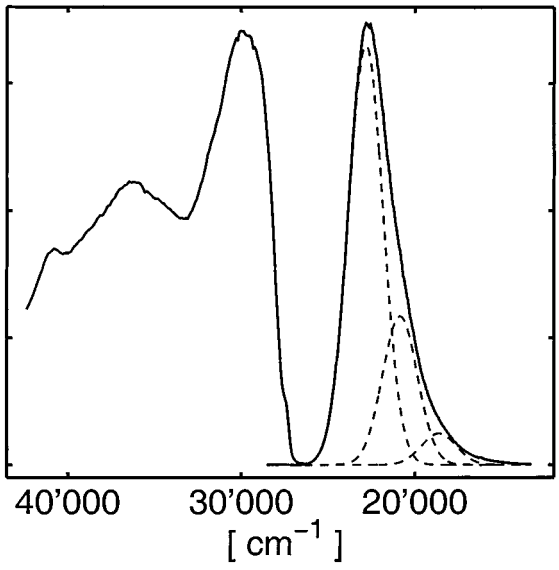

(a)

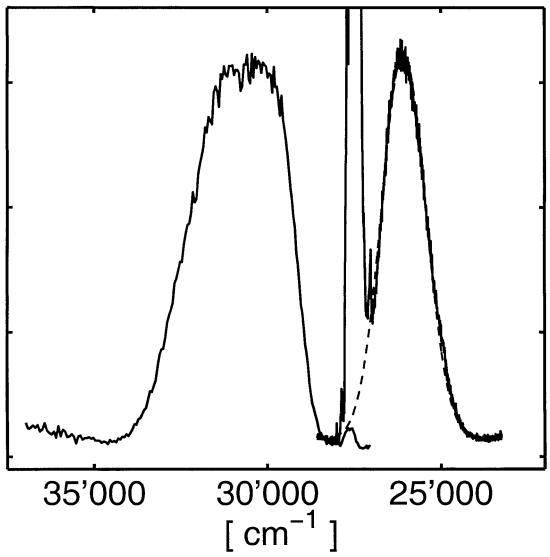

(b)

Figure 4. (a) Optical emission spectrum with excitation at 31 200 cm^{-1} and excitation spectrum with detection at 24 700 cm^{-1} of a $Ba_{12}F_{19}Cl_5$:Eu (1‰) single crystal ($T = 80$ K). The emission band was decomposed into three Gaussians of equal widths (dashed lines). (b) Optical emission and excitation spectrum of BaFCl:Eu^{2+} ($T = 80$ K). Luminescence excited at 29 325 cm^{-1}. Excitation spectrum detected at 26 180 cm^{-1}. Also shown is the Gaussian (dashed curve) used to fit the d–f emission band. The f–f emission peaks are ∼100 times stronger.

4.2. Optical experiments

We assign the broad emission band to $4f^6 5d \rightarrow 4f^7$ transitions of the Eu^{2+} ions, similar to the situation in many Eu^{2+} doped alkali and alkaline earth halide and double halide crystals

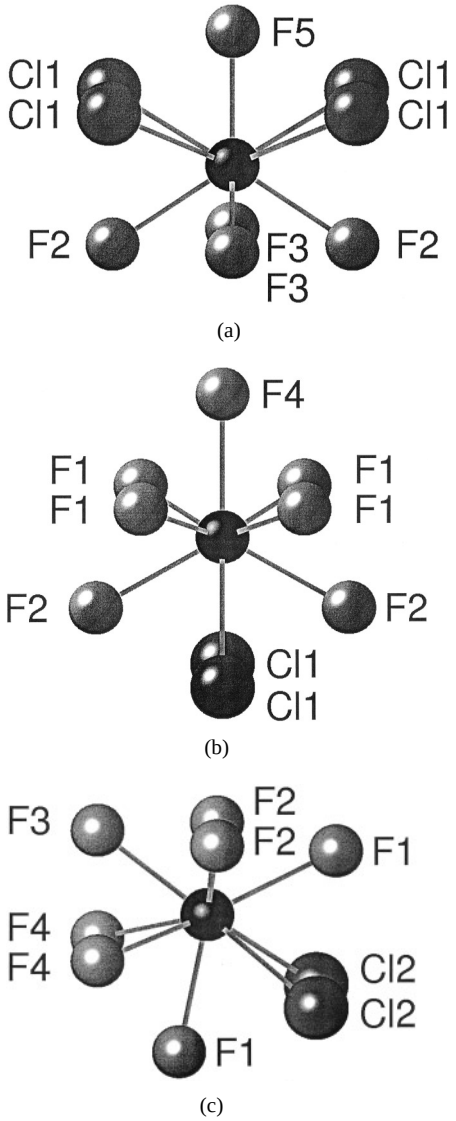

Figure 5. The different host cation environments in the perfect $Ba_{12}F_{19}Cl_5$ structure. In each case the (*ab*) mirror plane is parallel to the paper and contains the central barium cation. (a) Local coordination (A), point symmetry C_{2v} (see text); (b) local coordination (B), point symmetry C_{2v} (see text); (c) local coordination (C) point symmetry C_s (see text).

(see [18] and references therein). The band shows an ill resolved structure but can be completely decomposed into three Gaussians (see figure 4(a)). Figure 4(b) further shows for comparison the excitation–emission spectrum of $BaFCl:Eu^{2+}$ (one single cation lattice site as confirmed by EPR) recorded at ∼80 K [17, 19, 20]. This emission spectrum consists of one very nearly Gaussian curve superposed by the well known f–f transitions between 27 300 and 27 600 cm^{-1}. By assuming that each one of the three Eu^{2+} centres in the $Ba_{12}F_{19}Cl_5$ structure contributes only one d–f emission band three Gaussians can be assigned to the three sites. It is well known that the ligand field has stronger effects on the 5d levels than on the 4f ones and it can be expected

that the $4f^6 5d^1$ configurations of the three centres are affected mutually differently. The structure of the excitation spectrum is probably much more difficult to interpret as the complex level structure is determined by several factors: the mutually not strongly separated multiplets of the configuration $(4f^6(^7F_J), 5d^1)$ (total splitting $\sim$1100 cm^{-1}), the important ligand field and the comparatively strong electron–phonon coupling ($S > 24$ for the observed bands). As no intra-f-shell $^6P_{7/2} \rightarrow ^8 S_{7/2}$ transitions were observed (in contrast to the BaFCl:Eu^{2+} case, figure 4(b)) the $4f^6 5d^1$ level structure reaches energies below the lowest excited $4f^7$ terms for all three centres.

5. Conclusion

The EPR and luminescence studies presented above show that the $Ba_{12}F_{19}Cl_5$ compound doped with 1 mol‰ EuF_2 leads to three different Eu^{2+} centres. Two of them have orthorhombic point symmetry while the last one is monoclinic. The association between the Eu^{2+} EPR spectra and the barium lattice sites has been partly possible, thanks to symmetry arguments. All of the Eu^{2+} EPR centres show an important ground state splitting. A ligand field of this importance tends to lower the bottom of the $4f^6 5d$ band and promotes the inter-configuration $4f^7 \leftarrow 4f^6 5d^1$ emission [21]. As a result, the Eu^{2+} ions in the $Ba_{12}F_{19}Cl_5$ host do not show f–f transitions at 80 K in contrast to the BaFCl case where the comparatively weak ligand field allows their observation.

Acknowledgments

The authors thank S Beuchat, D Frauchiger and F Rouge for technical help. This work was supported by the Swiss Priority Program Optics 2 and the Swiss National Science Foundation.

References

[1] Kaminskii A A 1990 *Laser Crystals (Springer Series in Optical Sciences 14)* (Berlin: Springer)
[2] Pilbrow J R 1990 *Transition Ion Electron Paramagnetic Resonance* (Oxford: Clarendon)
[3] Jaaniso R and Bill H 1991 *Europhys. Lett.* **16** 569
[4] Lakshmanan A R 1996 *Phys. Status Solidi* a **153** 3
[5] Blasse G 1993 *J. Alloys Compounds* **192** 17
[6] Hangleiter T, Koschnick T K, Spaeth J M, Nuttall R H D and Eachus R S 1990 *J. Phys.: Condens. Matter* **2** 6837
[7] Mori N and Oikawa T 1998 *Adv. Imaging Electron Phys.* **99** 241
[8] Kubel F, Hagemann H and Bill H 1996 *Z. Anorg. (Allg.) Chem.* **622** 343
[9] Kubel F, Bill H and Hagemann H 1999 *Z. Anorg. (Allg.) Chem.* **625** 643
[10] Rey J M, Bill H, Lovy D and Hagemann H 1998 *J. Alloys Compounds* **268** 60
[11] Stevens K W H 1952 *Proc. Phys. Soc.* **65** 209
[12] Abragam A and Bleaney B 1970 *Electron Paramagnetic Resonance of Transition Ions* (Oxford: Oxford University Press)
[13] Rey J M, Bill H, Lovy D and Hagemann H 1998 *J. Alloys Compounds* **274** 164
[14] Sauvage M 1974 *Acta Crystallogr.* B **30** 2786
[15] Nicollin D and Bill H 1976 *Solid State Commun.* **20** 135
[16] Nicollin D and Bill H 1978 *J. Phys. C: Solid State Phys.* **11** 4803
[17] Nicollin D 1979 Etude d'ions à l'états S dans des monocristaux à structure en couche *Thesis* 1831, University of Geneva
[18] Rubio J 1991 *J. Phys. Chem. Solids* **52** 101
[19] Tanguy B, Merle P, Pezat M and Fouassier C 1974 *Mater. Res. Bull.* **9** 831
[20] Sommerdijk J L, Verstegen J M P J and Bril A 1974 *J. Lumin.* **8** 502
[21] Fouassier C, Latourette B, Portier J and Hagenmuller P 1976 *Mater. Res. Bull.* **11** 933